Indian Journal of Pure & Applied Physics
Vol. 52, May 2014, pp. 341-347

Synthesis and characterization of polyaniline/TiO_2 composites

Asha[1], Sneh Lata Goyal[1]*, D Kumar[2], Shyam Kumar[3] & N Kishore[1]

[1]Department of Applied Physics, Guru Jambheshwar University of Science and Technology, Hisar 125 001, Haryana, India

[2]Department of Chemistry, Guru Jambheshwar University of Science and Technology, Hisar 125 001, Haryana, India

[3]Department of Physics, Kurukshetra University, Kurukshetra 132 119, Haryana, India

*E-mail: goyalsneh@yahoo.com

Received 11 April 2013; revised 9 December 2013; accepted 12 February 2014

The synthesis and characterization of polyaniline (PANI)/TiO_2 polymer composites have been studied. The synthesis method is based on chemical oxidative polymerization of aniline added with various weight % of TiO_2 in the presence of ammonium persulphate as an oxidant. The results of XRD confirm the presence of TiO_2 in the composites. The FTIR shows systematic shifting of the characteristic bands of PANI with the increase in content of TiO_2. The SEM images revealed uniform distribution of TiO_2 particles in the PANI matrix. The evaluation of the dynamical parameters for PANI/TiO_2 composites using technique such as TGA has been reported. The thermal stability of composites increases with the increase in TiO_2 weight %. Although PANI/TiO_2 composites show lower *dc* electrical conductivity as compared to PANI and the conductivity decreases with increasing content of TiO_2, but they show a higher thermal stability than that of PANI. Further, the *dc* electrical conductivity is observed to increase with the increase in temperature. This work opens new perspectives for the use of PANI/TiO_2 composites as a conducting material at high temperatures.

Keywords: Polyaniline, XRD, SEM, DSC/TGA/DTA, FTIR, *dc* Conductivity, TiO_2

1 Introduction

Most of the polymers reported in literature are insulators. But after the synthesis of polyacetylene by Shirakawa *et al*[1]., it has been shown that polymers can also exhibit semiconducting behaviour. Polymers possess unique optical, electronic and mechanical properties and thus have potential applications which covers a broad spectrum including sensors[2,3], electro chromic display devices[4], electromagnetic interference (EMI) shielding[5-12], electrostatic charge dissipation[13] (ESD), rechargeable batteries[14,15], anti-corrosive coatings[16,17], removal of toxic ions and in the fabrication of light emitting diodes[18,19]. Besides other conducting polymers, polyaniline (PANI) has been extensively studied due to its non-redox doping, good environmental and thermal stability[20], high conductivity and economic feasibility[8]. In particular, the PANI filled with materials like magnetic particles[10,21,22] (e.g. Fe_2O_3, Fe_3O_4, $BaFe_{12}O_{19}$ etc.) or dielectric particles[3,5,10,23-25] (e.g. $BaTiO_3$, TiO_2, $SrTiO_3$ etc.) or carbonaceous fillers[6-9,11,26] (carbon black, graphite, carbon nanotubes, graphene etc.) display combination of dielectric/magnetic and electrical properties. Such composites have been demonstrated for applications in the area of microwave absorption[7,13,21,22,26] supercapacitors[13], corrosion control[8,27] etc. Later on, it was shown that the conductivity of PANI changes significantly[25] upon adding TiO_2. Subsequently, efforts have been made to improve the conducting properties of these materials.

In composite form, the properties of PANI change significantly. Till now, a number of studies on composites of PANI/TiO_2 have been reported[23-25] and majority of the researchers are still focusing on their synthesis and characterization. Detailed study with varying amounts of TiO_2 in PANI using different techniques has been carried out.

In the present paper, the synthesis of PANI/TiO_2 composites with different concentrations of TiO_2 is reported. The characterization of all these samples has been performed using X-ray diffraction (XRD), scanning electron microscopy (SEM), Fourier transform infrared (FTIR) spectroscopy and thermal analysis. The variation in *dc* conductivity of these composites has also been studied as a function of temperature and concentration.

2 Experimental Details

2.1 Synthesis of PANI

To prepare PANI, 0.2 M aniline hydrochloride (Aldrich) was oxidized with 0.25 M ammonium persulphate (Aldrich) in aqueous medium. For this, both the solutions were left to cool in the refrigerator for 2-3 h and then mixed in a beaker drop-wise,

keeping temperature between 0-4°C in an ice bath, stirred for 2 h and left for 24 h at rest to polymerize in refrigerator. Thereafter, PANI precipitate was collected on a filter paper and washed with 1 M HCl and acetone till the filtrate turned colourless. PANI (emeraldine) hydrochloride powder was dried in air and then in vacuum at 45°C. PANI prepared under these conditions was taken as standard sample.

2.2 Preparation of PANI/TiO_2 composites

The different compositions of PANI and titanium dioxide (TiO_2) composites were prepared by adding 20, 40 and 50 weight percentage of titanium dioxide (Aldrich) to 0.2 M aniline hydrochloride solution in distilled water before oxidizing by vigorous stirring for 2 h in order to keep the titanium dioxide powder suspended in the solution. Following this procedure, three different PANI/TiO_2 composites were prepared and named as t20, t40 and t50, respectively depending on the amount (weight %) of added TiO_2.

2.3 Analytical techniques

The samples were characterized by XRD, SEM, FTIR and TGA techniques. XRD studies of the samples were performed by using Rigaku Table-Top X-ray diffractometer. SEM was performed using Microtrac Semtrac Mini Scanning Electron Microscope (SM-300). FTIR analysis was done using Shimadzu IR affinity-1 8000 FTIR spectrophotometer by mixing the powder sample with dry KBr. TGA analysis was performed by TA instrument, model no. SDT Q600 in nitrogen atmosphere with a heating rate of 10°C/min. The *dc* conductivity measurements were made by using Keithley 6517A electrometer.

3 Results and Discussion

3.1 XRD analysis

The XRD patterns of the pure PANI, TiO_2 and PANI/TiO_2 composites, synthesized by doping TiO_2 into PANI during polymerization method are shown in Fig. 1. Perusal of the Fig. 1 shows that the XRD pattern of PANI has broad band at a value of $2\theta \approx 25$ degrees and titanium dioxide has sharp peak of maximum intensity at 25.38 degree along with certain other peaks of low intensity. The observed 2θ values of the peaks are consistent with the standard JCPDS values (JCPDS No. 4-0477).

XRD patterns of PANI/TiO_2 composites exhibit the presence of titanium dioxide in polyaniline. The intensity of diffraction peaks of these composites

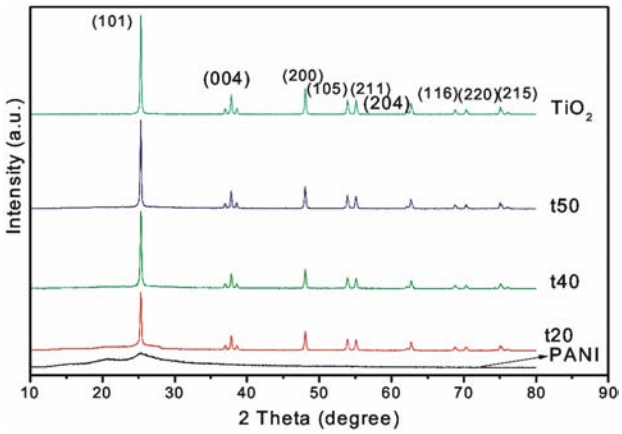

Fig. 1 — XRD patterns of PANI, TiO_2 and PANI/TiO_2 composites

increases as expected with increasing content of titanium dioxide.

The average crystallite size of TiO_2 and PANI/TiO_2 composites has been calculated using the Scherrer's formula[28]:

$$D = \frac{K\lambda}{\beta \cos\theta} \quad \ldots (1)$$

where D is crystallite size, λ is the X-ray wavelength (of Cu K_α used in the present study), K(=0.89) is the shape factor, $\cos\theta$ is the cosine of the Bragg angle (θ) and β is the full width at half of diffraction peak in radians. Eq. (1) when applied for the characteristic (101 plane) peak of TiO_2 and its composites with PANI lead to an average size of about 35 nm.

3.2 FTIR analysis

Figure 2 shows the FTIR spectra of PANI, PANI/TiO_2 composites and pure TiO_2. The FTIR spectrum of PANI shows characteristic vibrations in the region 1000-1500 cm^{-1}. It shows characteristic bands at 520, 815, 1163, 1317, 1495 and 1589 cm^{-1}. The bands at 520 and 815 cm^{-1} are due to C-H out-of-plane bending vibration and *para*-disubstituted aromatic rings, respectively[19]. A band appearing near 1317 cm^{-1} represents the C-N stretching vibration[19]. In plane bending vibration[11] in C-H occurs at 1163 cm^{-1}. The presence of bands in the range 1450-1600 cm^{-1} is attributed to non- symmetric C_6 ring stretching modes[19].

The higher frequency vibration at 1589 cm^{-1} has a major contribution from the quinoid rings, while the lower frequency mode at 1495 cm^{-1} shows the presence of benzenoid ring units. The broad band

observed at 2400-2750 cm^{-1} is due to aromatic C-H stretching vibrations while the band at 2950-3300 cm^{-1} is attributed to N-H stretching of aromatic amines[25].

In TiO_2, broad bands around 636 cm^{-1} and 3750 cm^{-1} correspond to Ti-O-Ti and O-H stretching frequencies[23], respectively. In case of composites of PANI/TiO_2, there exists small shifting in frequencies of PANI bands. In PANI/TiO_2 composites the bands of TiO_2 are also visible. Thus, the FTIR results confirm the presence of TiO_2 in the composites.

3.3 Thermo gravimetric analysis (TGA)

TGA thermo grams of PANI and PANI/TiO_2 composites in nitrogen atmosphere are shown in Fig. 3 while Differential Thermo Gravimetric (DTG) thermo grams are shown as inset in Fig. 3. The TGA and DTG analysis of PANI/TiO_2 composites indicate the four steps of weight loss.

(1) First stage starting at about 100°C is considered as initial dehydrating stage and due to desorption of water absorbed at the surface of doped polymer[23].

(2) Second stage at about 250°C is due to removal of protonic acid component[23].

(3) The following stages (third at about 500°C and fourth at about 600°C) indicate the polymer chain break which can lead to production of gases[29].

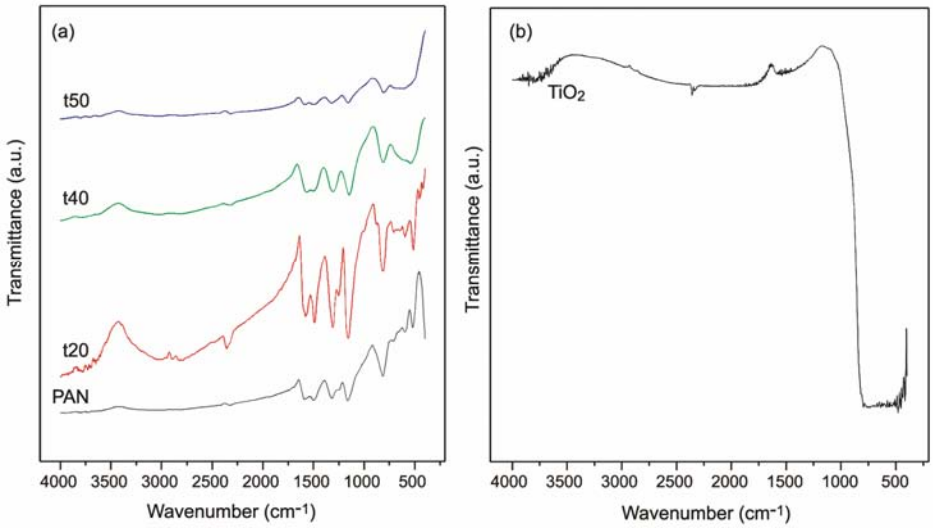

Fig. 2 — FTIR spectra of (a) PANI and PANI/TiO_2 composites and (b) TiO_2

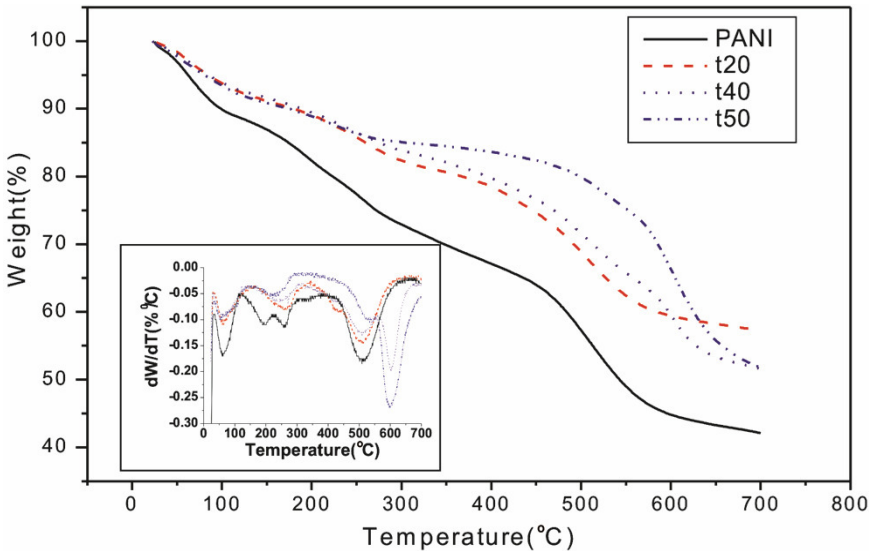

Fig. 3 — TGA and DTG (inset) thermo grams of PANI and PANI/TiO_2 composites

3.3.1 Activation energy

The activation energy of pure PANI and PANI/TiO_2 composites has been deduced using the expression[30]:

$$\ln\left[\ln\left(\frac{w-w_o}{w-w_f}\right)\right]=\frac{E_a\theta}{RT_s^2} \qquad \ldots(2)$$

where w_0 is the initial weight, w is the remaining weight at temperature T, w_f is the final weight, E_a is the activation energy, R is gas constant and $\theta = T-T_s$ with T_s as the reference temperature corresponding to $[(w-w_o)/(w-w_f)]=1/e$.

From Eq. (2), the activation energy E_a can be calculated from the slope of the linear fitted line between ln $\{\ln[(w-w_o)/(w-w_f)]\}$ and θ as shown in Fig. 4 for pure PANI and PANI/TiO_2 composites.

The values of activation energy so obtained have been listed in Table 1. It is clear that the value of activation energy increases with increasing content of TiO_2. This increase may be due to increase in packing density and reorganization of molecular arrangements etc. in the polymeric sample which signifies the increase in thermal stability of the polymer[31-34].

3.3.2 Frequency factor

Frequency factor is a constant indicating how many collisions have the correct orientation to lead to products and is related to rate of reaction. The values of frequency factor for pure PANI and its composites with TiO_2 have been determined by substituting the values of the corresponding activation energy (E_a) in the expression[30,34]:

$$A=\frac{\beta E_a}{RT_s^2}\exp\left(\frac{E_a}{RT_s}\right) \qquad \ldots(3)$$

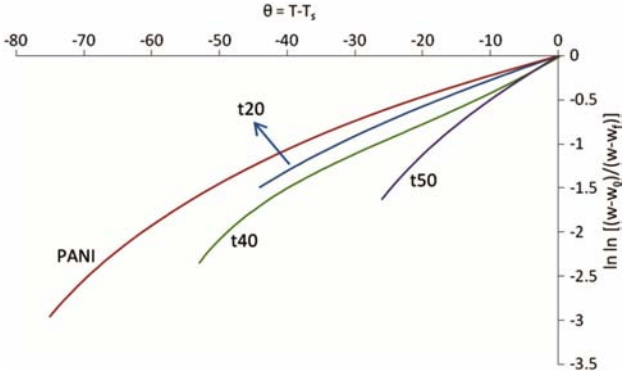

Fig. 4 — Plot of ln$\{\ln[(w-w_o)/(w-w_f)]\}$ vs. θ for PANI and PANI/TiO_2 composites

where A is the frequency factor and β is the constant rate of heating and other letters have their usual meanings. The calculated values of frequency factor are listed in Table 1. It is clear that corresponding to the decrease in values of activation energy, the values of frequency factor are observed to increase. This increase in the frequency factor shows that there is an increase in the rate of reaction. This may be due to the scissoning of the polymeric chains which increases the rate of reaction as the concentration of TiO_2 increases[32, 34].

3.3.3 Entropy of activation

The difference between the entropy of the transition state and the sum of the entropies of the reactants is called entropy of activation (ΔS) and is calculated as[34,35]:

$$\Delta S = 2.303\, R\log\left(\frac{Ah}{kT_s}\right) \qquad \ldots(4)$$

where h is Planck's constant and k is Boltzmann constant and other letters have their usual meanings. The values of entropy of activation so calculated are listed in Table 1. The value of entropy of activation increases with the increase in added concentration of TiO_2 which in turn suggests the increase in the rate of reaction[34]. Further, the negative value of ΔS indicates that the activated complex has more ordered structure than the reactants[35].

3.3.4 Free energy of change of decomposition

Free energy of change of decomposition (ΔG) is the difference between the enthalpy of the transition state and the sum of the enthalpies of the reactants in the ground state. It may be considered to be the driving force of a chemical reaction. ΔG determines the spontaneity of the reaction[34]. The values of ΔG are calculated using the expression[34,35]:

$$\Delta G = E_a - T_s\Delta S \qquad \ldots(5)$$

The values thus calculated are listed in Table 1. The positive values of ΔG signify the non-spontaneity of the degradation reaction[34].

Table 1 — Values of various kinetic parameters for PANI and PANI/TiO_2 composites

Sample	E_a (KJ/mol)	A (10^{10}) (s^{-1})	ΔS (J/mol/K)	ΔG (KJ/mol)
PANI	136.714	0.0926	–187.568	286.393
t20	151.230	0.2065	–172.283	289.229
t40	191.057	8.154	–103.548	281.455
t50	220.599	382.0	–30.1080	247.184

3.4 *dc* Conductivity

Voltage (*V*)–current (*I*) characteristics of PANI and various composites with TiO_2 at room temperature are shown in Fig. 5 here, as *V-I* characteristics of composite (having 20 wt. % of TiO_2) at different temperatures are shown in Fig. 6. The current increases non-linearly with applied voltage and the conduction mechanism in conducting polymers is very much different from intrinsic semiconductors[36]. In conducting polymers, the negative and positive charges initially added to the polymer chain do not simply begin to fill the rigid conduction or valence bands. In conducting polymers, there are no permanent dipoles. In fact, there exist random charge (polaron) trapping sites in the sample.

Under the influence of applied external field, a strong coupling between electrons and phonons causes lattice distortions around the added charge and hence, charge trapping becomes strong and their localized motion serves as an effective electric dipole. This leads to formation of quasi-particles such as polarons and bi-polarons. Here the charge transport is through these polarons and bi-polarons. As the applied field increases the formation of polarons and bi-polarons increases which contributes to the rapid increase in current with respect to voltage, resulting in non- linear curve[37].

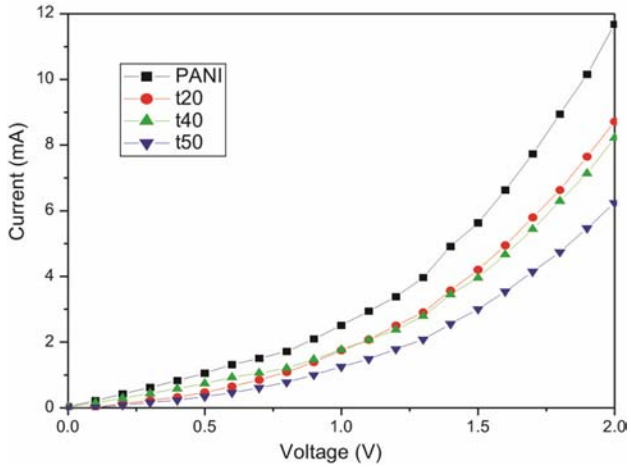

Fig. 5 — *I-V* characteristic of PANI and PANI/TiO_2 composites at room temperature (313 K)

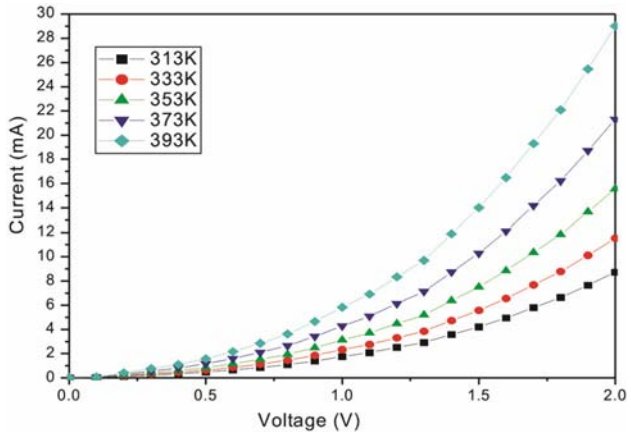

Fig. 6 — *I-V* characteristic of t20 sample at various temperatures

From the measured *V-I* characteristics of these samples, the values of *dc* electrical conductivity (σ) have been estimated at different temperatures at 1V:

$$\sigma = \frac{lXL}{VXA} \quad \ldots (6)$$

where *I* is the current, *L* the thickness, *V* the voltage and *A* is the area of cross-section of the sample. Table 2 indicates that the *dc* conductivity decreases on addition of TiO_2 and conductivity further decreases with increasing content of TiO_2 in PANI/TiO_2 composites[24,25]. This reduction in conductivity arises because electrons from polar O^{2-} terminated TiO_2 particle surfaces are transferred to PANI chains, resulting in their reduction. In a highly reduced PANI, as conjugation is lost, therefore, charges can get strongly localized in the PANI ring[24]. As shown in Fig. 7, the *dc* electrical conductivity increases with increase in temperature. This may be due to increase in free charges with increase in temperature[19].

The temperature dependence of the conductivity σ (*T*) of disordered semi-conducting materials is, generally, described by the Mott's variable range hopping (VRH) model, which is another possible charge transport mechanism in conducting polymers. Mott's VRH mechanism is a phonon assisted quantum-mechanical transport phenomena in which the movement of charge carriers to a nearby localized state of different energy is explained through the thermodynamic procedures, where as the movement of a charge carriers to a farther off localized state of similar energy is given by quantum mechanical

Table 2 — *dc* conductivity of PANI and PANI/TiO_2 composites at various temperatures at 1V

Temp (K)	Conductivity (10^{-4}) (S/cm)			
	PANI	t20	t40	t50
313	1.91	1.71	1.39	1.06
333	2.10	1.88	1.58	1.31
353	2.42	2.20	1.86	1.51
373	2.73	2.47	2.05	1.76
393	2.91	2.76	2.30	1.99

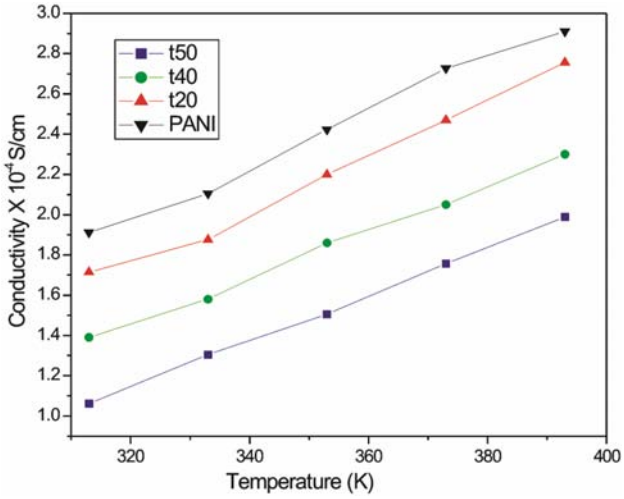

Fig. 7 — Temperature dependent *dc* conductivity of PANI and PANI/TiO_2 composites

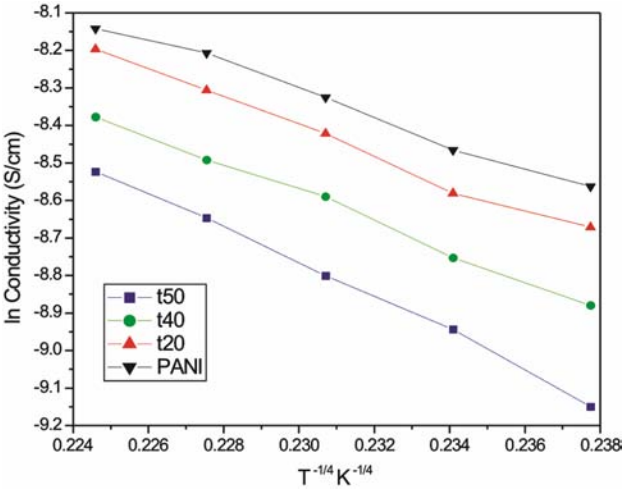

Fig. 8 — Plot of ln(σ) versus $T^{-1/4}$ of pure PANI and PANI/TiO_2 composites

Table 3 — Values of $\ln\sigma_0$ and T_0

Sample	$\ln\sigma_0$ (S/cm)	T_0 (10^6) K
PANI	–0.6052	1.255
t20	0.1573	1.904
t40	0.2869	2.211
t50	2.1098	5.034

tunneling[38]. The details worked out on this process leads to a characteristic temperature dependence of conductivity of the form $\ln\sigma(T)\alpha T^{[-1/(1+d)]}$, where σ is the conductivity of the sample and T is the temperature. Mott's model for hopping is given by:

$$\sigma(T) = \sigma_0 \exp\left[-\left(\frac{T_0}{T}\right)^{\gamma}\right] \quad \ldots (7)$$

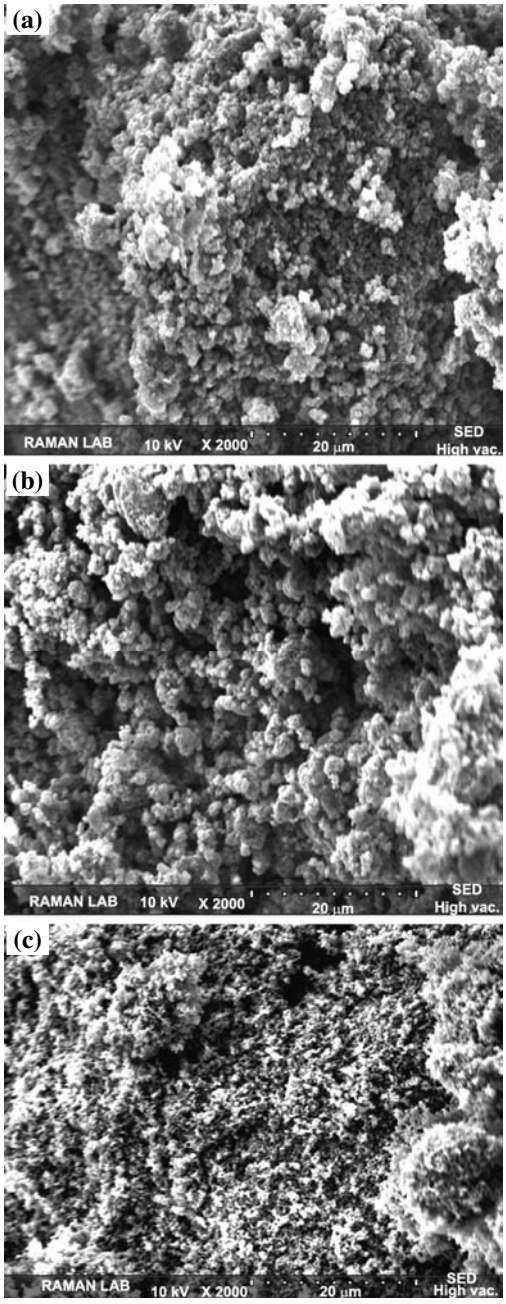

Fig. 9 — SEM micrographs of (a) Pure PANI (b) t50 and (c) TiO_2

where σ_0 is the high temperature limit of conductivity, T_0 is the Mott's characteristic temperature associated with the degree of localization of the electronic wave function. The exponent $\gamma=1/(1+d)$ determines the dimensionality of the conducting medium[39]. The possible values of γ are 1/4, 1/3 and 1/2 for three, two and one-dimensional systems, respectively[25]. The plot of $\ln\sigma(T)$ versus $T^{(-1/4)}$ is a straight line as shown in Fig. 8 indicating that three dimensional (3D) charge transport occurs in all the samples. The values of T_0

and $\ln\sigma_0$ obtained from the slopes and intercept are obtained from the above mentioned plots and shown in Table 3.

3.5 Scanning Electron Microscopy (SEM)

Typical SEM images for pure PANI, pure TiO_2 and PANI/TiO_2 composite (t20) are shown in Fig. 9. Perusal of SEM images shows that there is no agglomeration of TiO_2 particles in PANI matrix, rather there is uniform distribution of particles in the PANI matrix. Accordingly, it was considered that the TiO_2 particles are embedded within the structure built by PANI chains and generated the porous PANI/TiO_2 composites. It shows that it is easy to control the composite structure by using various types and shapes of metal oxides[19,40].

4 Conclusions

PANI and PANI/TiO_2 composites were synthesized by means of the oxidative polymerization of aniline hydrochloride in the presence of different wt% of TiO_2 with ammonium persulphate. The FTIR results confirm the presence of PANI in the composite and in case of composites of PANI/TiO_2, there exists small shifting in frequencies of the bands as observed in PANI. The SEM study of PANI-TiO_2 composites revealed uniform distribution of TiO_2 particles in PANI matrix. Although PANI/TiO_2 composites show lower *dc* electrical conductivity as compared to PANI, and it decreases regularly with increasing content of TiO_2. But the composites show a higher thermal stability than that of pure PANI, which can also be shown by comparing values of activation energy. The *dc* electrical conductivity of PANI and PANI/TiO_2 composites increases with increase of temperature. This work opens new perspectives for the use of PANI/TiO_2 composites as a conducting material at high temperature.

Acknowledgement

Authors are thankful to IRDE, Dehradun and DST (FIST), New Delhi for financial assistance in the form of grants.

References

1 Shirakawa H, Lewis E J, MacDiarmid A G, Chiang C K & Heeger A J, *J Chem Soc Chem Commun,* 16 (1977) 578.
2 Saini P & Arora M, *New Polymers for Special Applications* by Gomes A D (ed) Intech, Croatia, 2012.
3 Jumali M H H, Izzuddin I, Ramli N, Salleh M H & Yahaya M, *Solid State Sci Tech*, 17 (2009) 126.
4 Schnitzler D C & Zarbin A J G, *J Braz Chem Soc*, 15 (2004) 378.
5 Saini P, Arora M, Gupta G, Gupta B K, Singh V N & Choudhary V, *Nanoscale,* 5 (2013) 4330.
6 Saini P & Arora M, *J Mater Chem A*, 1 (2013) 8926.
7 Saini P, Choudhary V, Singh B P, Mathur R B & Dhawan S K, *Mater Chem Phys*, 113 (2009) 919.
8 Saini P, Choudhary V & Dhawan S K, *Polym. Advan.Technol*, 20 (2009) 355.
9 Maiti S, Shrivastava N K, Suin S & Khatua B B, *ACS Appl Mater Interfaces*, 5 (2013) 4712.
10 Saini P, Choudhary V, Vijayan N & Kotnala R K, *J Phys Chem C*, 116 (2012) 13403.
11 Saini P & Choudhary V, *J Nanoparticle Res,* 15 (2013) 1415.
12 Saini P & Choudhary V, *J Mater Sci*, 48 (2013) 797-804.
13 Saini P, Choudhary V & Dhawan S K, *Polym Advan Technol*, 23 (2012) 343.
14 Patil S D, Raghavendra S C, Revansiddappa M, Narsimha P, Ambika Prasad M V N, *Bull Material Science,* 30 (2007) 89.
15 MacDiarmid A G, Yang L S, Huang W S & Humphrey B D, *Synth Met*, 18 (1987) 393.
16 Wessling B, *Adv Mater,* 6 (1994) 226.
17 Lu W K, Elsenbaumer R L & Wessling B, *Synth Met,* 71 (1995) 2163.
18 Wang H L, MacDiarmid A G, Wang Y Z, Gebler D D & Epstein A J, *Synth Met,* 78 (1996) 33.
19 Chen S A, Chung K R, Chao C L & Lee H T, *Synth Met,* 82 (1996) 207.
20 Pud A, Ogurtsov N, Korzhenko A, & Shapoval G, *Prog Polym* Sci, 28 (2003) 1701.
21 Zhang B, Du Y, Zhang P, Zhao H, Kang L, Han X & Xu P, *J Appl Polym Sci,* 130 (2013) 1909.
22 Abbas S M, Chattterjee R, Dixit A K, Kumar A V R & Goel T C, *J Appl Phys, 101* (2007) 074105.
23 Ganesan R & Gedanken A, *Nanotechnology,* 19 (2008) 435709.
24 Pawar S G, Patil S L, Chougule M A, Raut B T, Jundale D M & Patil V B, *Archives of Appl Sci Res*, 2 (2010) 194.
25 Dey A, De S, De A & De S K, *Nanotechnology,* 15 (2004) 1277.
26 Saini P, Choudhary V, Singh B P, Mathur R B & Dhawan S K, *Synth Met*, 161 (2011) 1522.
27 Jeyaprabha C, Sathiyanarayanan S & Venkatachari, *J Appl Polym Sci*, 101 (2006) 2144.
28 Klug H P & Alex&er L E, *New York: Wiley,* 2 (1954) 491.
29 Dumitrescu I, Nicolae C A, Mocioiu A M, Gabor R A, Grigorescu M & Mihailescu M, *UPB Sci Bull,* 71 (2009) 63.
30 Horowitz H H & Metzger G, *Anal Chem*, 35 (1963) 1464.
31 Kalsi P C, Mudher K D S, P&ey A K & Iyer R H, *Thermochimica Acta,* 254 (1995) 331.
32 Anslyn E V & Dougherty D A, *Mod Physical Org Chem,* Edwards Brothers, Inc USA (2006).
33 Nouh S A, Atta M R & El-Melleegy W M, *Rad Effects & Defects in Solids,* 159 (2004) 461.
34 Gupta Renu, Kumar V, Goyal P K, Kumar Shyam, Kalsi P C & Goyal Sneh Lata, *Adv Appl Sci Res,* 2 (2011) 248.
35 Mallikarjun K G, *E-Journal of Chem*, 1 (2004) 105.
36 Reghu M, Cao Y, Moses D & Heeger A J, *Phys Rev B*, 47 (1993) 1758.
37 Jain N, Patidar D, Saxena N S & Sharma Kananbala, *Indian J Pure & Appl Phys,* 44 (2006) 767.
38 Maddison D S & Tansley T L, *J Appl Phys,* 72 (1992) 4677.
39 Shaktawat V, Jain N, Saxena R, Saxena N S, Sharma K & Sharma T P, *Polym Bull,* 57 (2006) 535.
40 Nabid M R, Golbabaee M, Moghaddam A B, Dinarv& R & Sedghi R, *Int J Electrochem Sci,* 3 (2008) 1117.